# Continuous measurements of stable isotopes of carbon dioxide and water vapor in an urban atmosphere: isotopic variations associated with meteorological conditions

**R. Wada[a,b], Y. Matsumi[a,c]*, T. Nakayama[a,c], T. Hiyama[a], Y. Fujiyoshi[d], N. Kurita[a], K. Muramoto[e], S. Takanashi[f], N. Kodama[g], Y. Takahashi[h]**

[a] *Institute for Space-Earth Environmental Research, Nagoya University, Nagoya 464-8601 Japan*

[b]*Department of Natural and Environmental Science, Teikyo University of Science, Uenohara 409-0193 Japan*

[c]*Graduate School of Science, Nagoya University, Nagoya, 464-8601, Japan*

[d]*Institute of Low Temperature Science, Hokkaido University, Sapporo 060-0819 Japan*

[e]*Kanazawa University, Kanazawa 920-1192 Japan*

[f]*Forestry and Forest Products Research Institute, Tsukuba 305-8687 Japan*

[g]*National Institute of Agro-Environmental Sciences, Tsukuba 305-8604 Japan*

[h] *National Institute for Environmental Studies, Tsukuba 305-8506 Japan*

29 January 2018

*Corresponding author

Institute for Space-Earth Environmental Research, Nagoya University, Furo-cho, Chikusa-ku, Nagoya, 464-8601, Japan

Tel: +81 52 747 6412

25 Fax: +81 52 789 5787

26 E-mail: **matsumi@nagoya-u.jp**

27

**Abstract**

Isotope ratios of carbon dioxide ($\delta^{13}C\text{-}CO_2$ and $\delta^{18}O\text{-}CO_2$) and water vapor ($\delta^{2}H\text{-}H_2Ov$ and $\delta^{18}O\text{-}H_2Ov$) in the near-surface air were continuously measured for one month in an urban area of the city of Nagoya in central Japan in September 2010 using laser spectroscopic techniques. During the passages of a typhoon and a stationary front in the observation period, remarkable changes in the isotope ratios of $CO_2$ and water vapor were observed. The isotopic ratios of both $CO_2$ and water vapor decreased during the typhoon passage. The decreases can be attributed to the air coming from an industrial area and the rainout effects of the typhoon, respectively. During the passage of the stationary front, $\delta^{13}C\text{-}CO_2$ and $\delta^{18}O\text{-}CO_2$ increased, while $\delta^{2}H\text{-}H_2Ov$ and $\delta^{18}O\text{-}H_2Ov$ decreased. These changes can be attributed to the air coming from rural areas and the air surrounding the observational site changing from a subtropical air mass to a subpolar air mass during the passage of the stationary front. A clear relationship was observed between the isotopic $CO_2$ and water vapor and the metrological phenomena. Therefore, isotopic information of $CO_2$ and $H_2Ov$ could be used as a tracer of metrological information.

**Keywords**

$CO_2$; Water vapor; Isotope; Laser spectroscopy; Typhoon, Stationary front

## 1. Introduction

Isotopic ratios of $CO_2$ are changed by emission and absorption processes such as biological respiration, combustion of fossil fuel and photosynthesis. Isotopic ratios of water vapor ($H_2Ov$) are also dependent on weather, climate and location, which are changed by evaporation and condensation processes. Therefore, the observation of $CO_2$ and $H_2Ov$ isotope compositions is a very powerful method to investigate the sources and dynamics of atmospheric $CO_2$ and $H_2Ov$ [1-5]. Takahashi et al. observed carbon isotope compositions of $\Delta^{14}C$ and $\delta^{13}C$ in atmospheric $CO_2$ and used them to estimate the contributions of fossil fuels and biogenic respiration [6,7]. Wada et al. observed $\delta^{13}C$ and $\delta^{18}O$ isotope compositions in atmospheric $CO_2$ in Nagoya, an urban city in Japan, and reported the subsequent contributions of natural gas combustion, petroleum combustion and biogenic respiration [8]. They also observed $\delta^{13}C$ and $\delta^{18}O$ isotope compositions in $CO_2$ with $\delta^{2}H$ and $\delta^{18}O$ in water vapor in a forest site and discussed the sources and dynamics of atmospheric $CO_2$ and $H_2Ov$ [9].

Studies of cyclones with observations of water vapor isotopes ($\delta^{2}H$-$H_2Ov$, $\delta^{18}O$-$H_2Ov$) have been reported [10-14]. Measurements of water vapor isotope ratios provide valuable information to understand the atmospheric hydrological cycle because stable isotope ratios are influenced by water vapor advection, condensation, and evaporation [15]. Lawrence et al. reported low values and inward decreases in the isotope ratios in the rain and vapor of four tropical cyclones [10]. They concluded that the low values of the isotope ratios were a result of the cyclone's size, longevity, and deep clouds and that the inward decrease was due to diffusive isotope exchange

between falling rain and converging vapor in the atmospheric boundary layer. Fudeyasu et al. observed the isotope ratios of precipitation and water vapor during the passage of a typhoon over Ishigaki Island, southwestern Japan, and found that isotope ratios of precipitation and water vapor decreased inward in the cyclone's outer region but increased in the cyclone's inner region [12]. Kurita et al. used a laser spectroscopic technique to observe water vapor isotope ratios in the city of Nagoya in central Japan and reported how the stationary front influenced the isotope variation in the precipitation [16].

Simultaneous and continuous measurements of stable isotope ratios of $CO_2$ and water vapor in urban areas are still scarce. The variations of stable isotope ratios of $CO_2$ and water vapor in meteorological events have not yet been adequately discussed. Isotope ratio mass spectrometry (IRMS) has been used as the conventional method to determine the isotopic composition with high accuracy; however it leads to low temporal data resolution. A laser spectroscopic method has the advantage of high temporal resolution.

In this study, we report continuous and in-situ measurements of $CO_2$ isotope ratios of $^{13}C/^{12}C$ and $^{18}O/^{16}O$ and water vapor isotope ratios of $^{2}H/^{1}H$ and $^{18}O/^{16}O$ with high temporal resolutions using laser spectroscopic methods in an urban area of the city of Nagoya in central Japan in September 2010. Remarkable changes in the isotope ratios during the passages of a typhoon and a stationary front are presented, and the relationships between the variations in the isotopic compositions and the meteorological data are discussed.

## 2. Materials and Methods

97 The measurement system used for the current observations have been described
98 elsewhere [8,9,16,17]; however a general description of the absorption spectrometers
99 and the key components is given here. A $CO_2$ isotope spectroscopic instrument
100 (Aerodyne Research Inc., USA, QC-TILDAS-ISO) was used. This instrument has the
101 capability to selectively analyze the three most abundant $CO_2$ isotopologues ($^{16}O^{12}C^{16}O$,
102 $^{18}O^{12}C^{16}O$, and $^{16}O^{13}C^{16}O$) in the wavelength of 2310 $cm^{-1}$ [18]. The concentrations of
103 $CO_2$ were observed using a $CO_2$ gas analyzer (LI-COR Inc., USA, LI-840).
104 Calibration is critical when the measured isotopic ratios are at a precision level of
105 0.1‰. We used two calibrations. The first calibration was to determine the dependence
106 of the measured isotopic ratios on the total $CO_2$ concentration [18]. Our instrument
107 showed a linear dependence of the measured isotopic ratios on the $CO_2$ concentrations,
108 with the dependence of the isotopic ratios about -4 ‰ when the concentration of $CO_2$
109 changed by +20 μmol $mol^{-1}$[8].
110 The first calibration was performed by introducing reference gases with
111 concentrations of 354 μmol $mol^{-1}$ and 443 μmol $mol^{-1}$, which were prepared by diluting
112 the standard gas ($\delta^{13}C$ = -12.6‰, $\delta^{18}O$ = -8.92‰, and $[CO_2]$ = 470 μmol $mol^{-1}$) with
113 $CO_2$-free air ($[CO_2]$ < 0.1 μmol $mol^{-1}$), to the instrument and measuring them for 2 min
114 each.
115 Another calibration was done at the beginning of the observation to calibrate the
116 offset and span of the measured isotopic ratios. A linear relationship between two
117 standard gases (gas A: $\delta^{13}C$ = -12.68‰, $\delta^{18}O$ = -9.71 ‰, $[CO_2]$ = 498 μmol $mol^{-1}$, and
118 gas B: $\delta^{13}C$ = -9.11‰, $\delta^{18}O$ = -7.07‰, $[CO_2]$ = 413 μmol $mol^{-1}$) was applied for the
119 calibration.

120 The isotopic ratios of the reference $CO_2$ were measured using dual inlet isotope
121 ratio mass spectroscopy (IRMS) at the National Institute for Environmental Studies
122 (NIES), Japan. Primary standards were supplied by NIES [19].The precisions of the
123 $\delta^{13}C$ and $\delta^{18}O$ measurements were estimated via an Allan variance analysis using
124 compressed air [20] at the observatory. The analysis showed that the precision of the
125 measurements was approximately 0.03‰ for both $\delta^{13}C$ and $\delta^{18}O$ over a period of 100
126 sec.
127 A water vapor isotope analyzer (WVIA, model DLT-100, Los Gatos Res. Inc., USA)
128 was used to measure the water vapor isotopes ($\delta^{2}H$ and $\delta^{18}O$) and the water vapor
129 concentration. The methodology employed was based on an off-axis integrated cavity
130 output spectroscopy system (OA-ICOS) using a diode laser with a wavelength of
131 approximately 1.39 μm. The laser wavelength was swept through the selected
132 absorption line for each species ($H_2O$, HDO, and $H_2{}^{18}O$). Data calibration for the water
133 vapor isotope measurements followed the method of Kurita et al. [17]. Standard air with
134 a known isotopic vapor content was generated using a Water Vapor Isotope Standard
135 Source (WVISS, Los Gatos Res. Inc.) in conjunction with the WVIA, which was
136 programmed to perform a calibration every 50 min after ambient air measurement.
137 Isotope compositions are indicated here as delta values [21]:
138
139 $$\delta = \left( \frac{R_{Sample} - R_{Standard}}{R_{Standard}} \right) \quad (‰), \qquad (2)$$
140
141 where $R_{Sample}$ is the molecular ratio of the heavy to light isotopologues in the sample air.
142 For the $R_{Standard}$ of $^{13}C/^{12}C$ in $CO_2$, the Vienna Pee Dee Belemnite (VPDB) scale was

used [22]. For the $R_{Standard}$ of $^{18}O/^{16}O$ in $CO_2$, the VPDB scale for $CO_2$ gas (VPDB-$CO_2$) was used. For the water vapor isotope ratios $\delta^2H$ and $\delta^{18}O$ in the air, the Vienna Standard Mean Ocean Water (VSMOW) scale was used.

Ambient air was sampled from the top of the Solar Terrestrial Environment Laboratory building at Nagoya University (35°09′N 136°58′E) through a 10 m Nylon tube (Nitta Corporation). There was an approximately 15-second time lag between pulling the ambient air from the top of the building and its arrival at the spectrometer. A PTFE membrane filter (pore size 1 μm) was inserted between the Nylon tubing and the spectrometer to prevent light-scattering aerosols from entering the instrument. We chose not to dry the ambient air to avoid fractionation or exchange during the drying procedure, which may be particularly relevant for $^{12}C^{18}O^{16}O$ [23]. The observation site was surrounded by vegetation but was located in a highly populated urban area of Nagoya, which is located at the center of main island of Japan with a population of 2.3 million.

Meteorological data such as wind speed and direction, air temperature, and precipitation, were obtained from the Nagoya Local Meteorological Observatory, which is ~1 km from the observation site.

## 3. Results

The observed $CO_2$ isotopic ratios, $\delta^{13}C$-$CO_2$, $\delta^{18}O$-$CO_2$, and the $CO_2$ concentration from September 1 to September 27, 2010 are shown in Fig. 1. The observed data for the $CO_2$ isotopes were averaged for each minute. The $CO_2$ concentration in the atmosphere ranged from 380 μmol $mol^{-1}$ to 480 μmol $mol^{-1}$ during the course of the observations, with carbon and oxygen isotopic compositions ranging from -14‰ to -10‰ VPDB for

167 $\delta^{13}C\text{-}CO_2$ and from -6‰ to 0‰ VPDB-$CO_2$ for $\delta^{18}O\text{-}CO_2$. The $CO_2$ concentrations,
168 $\delta^{13}C\text{-}CO_2$, and $\delta^{18}O\text{-}CO_2$ exhibited diurnal variations, with minimum $\delta^{13}C\text{-}CO_2$ and
169 $\delta^{18}O\text{-}CO_2$ values observed in the nighttime and maximum $\delta^{13}C\text{-}CO_2$ and $\delta^{18}O\text{-}CO_2$
170 values observed during the daytime. The variations in $\delta^{13}C\text{-}CO_2$ and $\delta^{18}O\text{-}CO_2$ were
171 nearly mirror images of the $CO_2$ concentration.

172 Figure 1 also shows the water vapor isotopic ratios, $\delta^{2}H\text{-}H_2Ov$, $\delta^{18}O\text{-}H_2Ov$, and the
173 water vapor concentration [$H_2Ov$] from September 1 to September 27, 2010. The
174 observed data for the water vapor isotopes were averaged for each 10 minutes. The water
175 vapor concentrations ranged from 9000 μmol $mol^{-1}$ to 30000 μmol $mol^{-1}$ over the course
176 of the investigation, with $\delta^{2}H\text{-}H_2Ov$ ranging from -170‰ to -90‰ VSMOW and
177 $\delta^{18}O\text{-}H_2Ov$ from -25‰ to -12‰ VSMOW. Diurnal variations in $\delta^{2}H\text{-}H_2Ov$ and
178 $\delta^{18}O\text{-}H_2Ov$ were not clear compared to the variations in $\delta^{13}C\text{-}CO_2$ and $\delta^{18}O\text{-}CO_2$. The
179 values of $\delta^{2}H\text{-}H_2Ov$ and $\delta^{18}O\text{-}H_2Ov$ during the one-month observation period had nearly
180 no long-term tendency, even though there were several abrupt decrease events.

181 Meteorological data (pressure, rainfall, temperature, wind speed, and wind direction)
182 are also shown in Fig. 1. Rainfall was observed on September 8, 15, and 23. During the
183 observation period, a typhoon and a stationary front passed over the observation site on
184 September 8 and 23, respectively.

185

186 **4. Discussion**

187 **4.1 Passage of the typhoon**

188 During the typhoon and stationary front passages in the observation period,
189 remarkable changes in the isotope ratios of $CO_2$ and water vapor were observed. The
190 9th typhoon of the year moved in from the west of the Honshu main island of Japan on

191 September 8. The track of the typhoon center is shown in Fig. 2, which was reported by
192 the Japan Meteorological Agency (JMA) [24]. The typhoon had a maximum
193 instantaneous wind velocity of 23 $ms^{-1}$ at 8:00 on September 8 when it was situated at
194 35°8′N 133°2′E. The typhoon moved to the east after the rainfall and passed over the
195 observation site on the morning of September 8. Our observation results on September 8
196 are shown in Fig. 3.

197 Before the typhoon passed over the observation site, the concentration of $CO_2$ was
198 ~390 μmol $mol^{-1}$, with approximately -10‰ for $\delta^{13}C$-$CO_2$ and -3‰ for $\delta^{18}O$-$CO_2$.
199 These observed values of $CO_2$ concentration and isotopic ratios of $CO_2$ were close to
200 that of the background air at mid-latitude. Before the passage of the typhoon, the
201 concentration of $H_2Ov$ was ~30000 μmol $mol^{-1}$ with approximately -100‰ for $\delta^{2}H$-$H_2O$
202 and -12‰ for $\delta^{18}O$-$H_2O$. The concentrations and isotopic ratios of $CO_2$ and water vapor
203 experienced large changes at approximately 10:00 on September 8. A large amount of
204 rainfall was observed at approximately 10:00 when the typhoon moved close to the
205 observation site. The concentration of $CO_2$ rapidly increased from 390 μmol $mol^{-1}$ to
206 420 μmol $mol^{-1}$, and the isotopic ratios of $CO_2$ decreased from -10‰ to -12‰ for
207 $\delta^{13}C$-$CO_2$ and from -2‰ to -4‰ for $\delta^{18}O$-$CO_2$. The surface air pressure decreased as the
208 typhoon approached the observation site and then increased after passing north of the
209 observation site at approximately 13:00. The wind speed had a maximum at
210 approximately 10:00. While the concentrations and isotopic ratios of $CO_2$ and water
211 vapor changed rapidly at approximately 10:00 with the strong rainfall, the pressure,
212 temperature, wind speed, and direction changed gradually.

213 To examine the source of the $CO_2$, which was responsible for the increase in the $CO_2$
214 concentration at approximately 10:00 on September 8, Keeling plot analyses of the $CO_2$

isotope ratios were performed. The intercept of the Keeling plots gives the isotope ratios of the source's $CO_2$ excess relative to the background atmospheric $CO_2$ [2]. The Keeling plots of $\delta^{13}C$-$CO_2$ and $\delta^{18}O$-$CO_2$ using observed data for 1 hour from 10:00 to 11:00 on September 8 are shown in Fig. 4. The Keeling plots of both $\delta^{13}C$-$CO_2$ and $\delta^{18}O$-$CO_2$ show good linearity. The intercept values of the Keeling plots of $\delta^{13}C$-$CO_2$ and $\delta^{18}O$-$CO_2$ are -24.2±0.5‰ and -19.9±0.9‰, respectively. The values of $\delta^{13}C$-$CO_2$ and $\delta^{18}O$-$CO_2$ are distinctive for sources such as petroleum combustion and biogenic respiration. The values of $\delta^{13}C$-$CO_2$ and $\delta^{18}O$-$CO_2$ for petroleum combustion have been reported in the ranges from -32‰ to -23‰, and from -18‰ to -15 ‰, respectively, and for biogenic respiration in the ranges from -30‰ to -25‰, and from -10‰ to +8‰, respectively [25]. Therefore, the intercept values of $\delta^{13}C$-$CO_2$ and $\delta^{18}O$-$CO_2$ in the Keeling plots in Fig. 4 indicate that the increase in the $CO_2$ concentration at approximately10:00 on September 8 was primarily due to anthropogenic $CO_2$ emission. Since several thermal electric power stations are located to the south of the observation site at distances of several tens of kilometers (Fig. 2), the air mass, including the $CO_2$ emitted from these power stations, might have been brought to the area of the observation site by the typhoon.

The decrease in the isotopic ratios of the water vapor was observed at approximately 10:00 in the inward stage of the typhoon, which was associated with strong rainfall (see Fig. 3). Fudeyasu et al. measured isotope ratios of water vapor during the passage of a typhoon over Ishigaki Island, Japan [12]. They observed a decrease in the water vapor isotope ratios with strong precipitation in the inward stage of the typhoon. They attributed the inward decrease in the isotope ratios of the water vapor to rainout effects, which involve both condensation efficiency, as reflected in inwardly increasing cloud

239 thickness, and isotopic exchange between falling droplets and ambient water vapor. The
240 decrease in the water isotope ratios observed in our study during the passage of the
241 typhoon (Fig. 3) could reflect the same phenomena as the results of Fudeyasu et al.
242 Since Fudeyasu et al. (2008) used a cryogenic sampling technique at an interval of 6 h
243 with laboratory IRMS analysis for the measurements of the water vapor isotopes, the
244 inward decrease in the water vapor isotope ratio was indicated by just one sampling
245 point [12]. However, we used a continuous in-situ technique with a laser spectroscopic
246 instrument; therefore, the inward decrease in the water vapor isotopes during the
247 typhoon event were more conspicuous, as shown in Fig. 3.

248 The increase in the $CO_2$ isotopes and the decrease in the water vapor isotopes were
249 observed simultaneously with the strong rainfall. It is likely that the $CO_2$ with lower
250 $\delta^{13}C\text{-}CO_2$ and $\delta^{18}O\text{-}CO_2$ values emitted from the industrial area located south of the
251 observatory were transported to the upper air above the observation site and then
252 descended with the subsidence flow owing to the rainfall.

253

254 **4.2 Passage of the stationary front**

255 A stationary front, called the autumnal rain (Akisame) front, passed over the
256 observatory on September 23, 2010. The Akisame stationary front is formed at the
257 transition zone between subtropical warm and subpolar cold air masses and is
258 characterized by a large gradient of equivalent potential temperature. The track of the
259 stationary front on September 23 is shown in Fig. 2, which was reported by the JMA.
260 The stationary front spread form east to west and moved from south to north past the
261 observation site. At 7:00 on September 23, 2010, the concentration of $CO_2$ was 440
262 μmol $mol^{-1}$ with -12 ‰ for $\delta^{13}C\text{-}CO_2$ and -4 ‰ for $\delta^{18}O\text{-}CO_2$ (Fig. 5). The high

263 atmospheric stability with relatively low wind speed may have contributed to the
264 relatively higher concentration of $CO_2$ before the passage of the stationary front because
265 $CO_2$ emitted from the surface might have remained near the surface. The concentration
266 of water vapor was ~27000 μmol $mol^{-1}$ with -100‰ for $\delta^2H$-$H_2Ov$ and -12‰
267 for $\delta^{18}O$-$H_2Ov$. At 7:30 on September 23, 2010, the concentrations and isotopic ratios of
268 the $CO_2$ and water vapor changed rapidly. The concentration of $CO_2$ decreased from
269 440 μmol $mol^{-1}$ to 400 μmol $mol^{-1}$, and the isotopic ratios of $CO_2$ increased from -12‰
270 to -10‰ for $\delta^{13}C$-$CO_2$ and from -4‰ to -2‰ for $\delta^{18}O$-$CO_2$. The surface air pressure
271 increased gradually after the passage. The temperature decreased rapidly when the
272 stationary front passed over the observation site at approximately 7:30; however it
273 increased again at 9:00 and decreased again after 10:30 with some fluctuations.
274 Interestingly, the wind speed increased rapidly at approximately 7:30, decreased just
275 after that, and then, increased again from 8:00 to 12:00 (Fig. 5). The concentration and
276 isotopic ratios of $H_2Ov$ showed minimum peaks at approximately 8:00, 11:30, and
277 14:00. Since rainfall events were observed at these times and the temperatures dropped
278 just after these events, the stationary front might have moved back and forth over the
279 observatory. The isotope ratios of water vapor, $\delta^2H$-$H_2Ov$ and $\delta^{18}O$-$H_2Ov$, decreased
280 rapidly at 7:30 and then fluctuated and finally settled to -150‰ for $\delta^2H$-$H_2Ov$ and -12‰
281 for $\delta^{18}O$-$H_2Ov$ at approximately 16:00. These results suggest that the temporal
282 variations of $\delta^2H$-$H_2Ov$ and $\delta^{18}O$-$H_2Ov$ were caused by the movement of the stationary
283 front. Schematic figures are shown in Fig. 6 to explain the positional relationships of the
284 observation site, power plants, and the stationary front before and after the stationary
285 front passed the observation site.

The Keeling plots of $\delta^{13}C\text{-}CO_2$ and $\delta^{18}O\text{-}CO_2$ using observed data for 1 hour from 7:00 to 8:00 on September 23, 2010 are shown in Fig. 7. The intercepts of the Keeling plots of $\delta^{13}C\text{-}CO_2$ and $\delta^{18}O\text{-}CO_2$ are -27.7±0.6‰ and -16.6±0.6‰, respectively. These intercepts indicate that the air mass with excessive high $CO_2$ concentration and low isotopic ratios due to the emission by anthropogenic sources was replaced by the background air mass which had low concentration and high isotopic values due to the passage of the stationary front.

While the isotope ratios of the water vapor on the surface are influenced by mesoscale meteorological conditions, such as air mass changes between subtropical marine air and subpolar air, convective downdrafts, and precipitations [16], the isotope ratios of $CO_2$ are affected by nearby local emissions and microscale weather in the boundary layer [6-9]. Relatively high $\delta^2H$ values of water vapor were observed at the observation site before the arrival of the stationary front from the north, which is characterized by a warm subtropical air mass with high $\delta^2H$ values of water vapor. Then, the abrupt $\delta^2H$ decreases in association with the passage of the stationary front may be due to the change to a northern subpolar air mass, which is characterized by low $\delta^2H$ values of water vapor. This is supported by back-trajectory calculations [26], which suggest that the air was transported from the ocean to the south of Honshu Island, Japan before the passage of the stationary front, and then the direction of the transported air mass changed towards the Asian continent in the northerly direction of Honshu Island.

## 5. Conclusions

A continuous in-situ observation of $CO_2$ and water vapor isotopes was successfully performed in an urban area of Nagoya for one month in September 2010. There were

two large rainfall events during the observation period, marking the passage of a typhoon on September 8 and a stationary front on September 26.

During the typhoon passage event, the concentration of $CO_2$ increased rapidly from 390 μmol $mol^{-1}$ to 420 μmol $mol^{-1}$, while $\delta^{13}C$-$CO_2$ and $\delta^{18}O$-$CO_2$ decreased with an inverse correlation to the $CO_2$ concentration in association with the strong rainfall. These changes were interpreted to indicate that air came from an industrial area into the upper air above the observation site, and then the air descended via subsidence flow with the rainfall. A Keeling plot analysis during the increase in the $CO_2$ concentration shows that $\delta^{13}C$-$CO_2$ and $\delta^{18}O$-$CO_2$ were -24.2‰ and -19.9‰, respectively. These values correspond to $\delta^{13}C$ and $\delta^{18}O$ values of anthropogenic $CO_2$, which may have been emitted from an industrial area to the south of the observation site. The decrease in the water vapor isotope ratios and the increase in the $CO_2$ isotope ratios are observed in association with strong rainfall and are attributed to rainout effects in the typhoon.

During the passage of the stationary front on September 23, the concentration of $CO_2$ decreased from 440 μmol $mol^{-1}$ to 400 μmol $mol^{-1}$. This decrease was interpreted as reflecting background air coming from a rural area located north of the observatory. A Keeling plot analysis showed that the $\delta^{13}C$-$CO_2$ and $\delta^{18}O$-$CO_2$ of the air during the decrease in the $CO_2$ concentration were -27.7‰ and -16.6‰, respectively. These intercepts indicate that the air mass containing anthropogenic $CO_2$ near the surface was replaced by a background clean air mass with low $CO_2$ concentration during the passage of the stationary front.

While the isotope ratios of water vapor on the surface are influenced by mesoscale meteorological conditions, such as air mass changes between subtropical marine air and subpolar air, convective downdrafts, and precipitations [16], the isotope ratios of $CO_2$

334 are affected by nearby local emissions and microscale weather in the boundary layer
335 [6-9].

336 We have discussed the relationship between the isotopic data of $CO_2$ and water vapor
337 and metrological information. Isotopic information of $CO_2$ and water vapor could
338 therefore be used as a tracer of metrological information.

339

340 **References**

341


342 [1] Mook WG. The effect of fossil fuel and biogenic $CO_2$ on the $^{13}C$ and $^{14}C$ content of
343 atmospheric carbon dioxide. Radiocarbon. 1980;22:392-397.

344 [2] Pataki DE, Bowling DR, Ehleringer JR. Seasonal cycle of carbon dioxide and its
345 isotopic composition in an urban atmosphere: Anthropogenic and biogenic effects. J
346 Geophys Res. 2003;108 (D23), 4735, doi:10.1029/2003JD003865.

347 [3] Pataki DE, Xu T, Luo YQ, Ehleringer JR. Inferring biogenic and anthropogenic
348 carbon dioxide sources across an urban to rural gradient. Oecologia. 2007;152:
349 307-322.

350 [4] Newman S, Xu X, Affek H, Stolper E, Epstein S. Changes in mixing ratio and
351 isotopic composition of $CO_2$ in urban air from the Los Angeles basin, California,
352 between 1972 and 2003. J Geophys Res. 2008;113, D23304,
353 doi:10.1029/2008JD009999.

354 [5] Gorski G, Strong C, Good SP, Bares R, Ehleringer JR, Bowen GJ. Vapor hydrogen
355 and oxygen isotopes reflect water of combustion in the urban atmosphere. PNAS.
356 2015;112:3247-3252.

[6] Takahashi H, Hiyama T, Konohira E, Takahashi A, Yoshida N, Nakamura T. Balance and behavior of carbon dioxide at an urban forest inferred from the isotopic and meteorological approaches. Radiocarbon. 2001;43:659-669.

[7] Takahashi HA, Konohira E, Hiyama T, Minami M, Nakamura T, Yoshida N. Diurnal variation of $CO_2$ concentration, $\Delta^{14}C$ and $\delta^{13}C$ in an urban forest: estimate of the anthropogenic and biogenic $CO_2$ contributions. Tellus B. 2002;54:97-109.

[8] Wada R, Pearce JK, Nakayama T, Matsumi Y, Hiyama T, Inoue G, Shibata T. Observation of carbon and oxygen isotopic compositions of $CO_2$ at an urban site in Nagoya using Mid-IR laser absorption spectroscopy. Atmos Environ. 2011;45:1168-1174.

[9] Wada R, Matsumi Y, Takanashi S, Nakai Y, Nakayama T, Ouchi M, Hiyama T, Fujiyoshi Y, Nakano T, Kurita N, Muramoto K, Kodama N. In situ measurement of $CO_2$ and water vapor isotopic compositions at a forest site using mid-infrared laser absorption spectroscopy. Isot Environ Health Stud. 2016;52:603-618.

[10] Lawrence JR, Gedzelman SD, Zhang X, Arnold R. Stable isotope ratios of rain and vapour in 1995 hurricanes. J Geophys Res. 1998;103: 11381-11400.

[11] Lawrence JR, Gedzelman SD, Gamache J, Black M. Stable isotope ratios: Hurricane Olivia. J Atmos Chem. 2002;41:67-82.

[12] Fudeyasu H, Ichianagi K, Sugimoto A, Yoshmura K, Ueta A, Yamanaka MD. Isotope ratios of precipitation and water vapour observed in Typhoon Shanshan. J Geophys Res. 2008;113:D12113 doi:10.1029/2007JD009313.

[13] Good SP, Mallia DV, Lin JC, Bowen GJ. Stable Isotope Analysis of Precipitation Samples Obtained via Crowdsourcing Reveals the Spatiotemporal Evolution of Superstorm Sandy. PLoS ONE. 2014;9:e91117. doi:10.1371/journal.pone.0091117.

[14] Munksgaard NC, Zwart C, Kurita N, Bass A, Nott J, Bird MI. Stable isotope anatomy of tropical cyclone Ita, North-Eastern Australia, April 2014. PLoS ONE. 2015;10:e0119728. Doi:10.1371/journal.pone.0119728.

[15] Lawrence JR, Gedzelman SD, White JWC, Smiley D, Lazov P. Storm trajectories in eastern US D/H isotopic composition of precipitation. Nature. 1982;296:638-640.

[16] Kurita N, Fujiyoshi Y, Wada R, Nakayama T, Matsumi Y, Hiyama T, Muramoto K. Isotopic variations associated with North-South displacement of the Baiu front. SOLA. 2013;9:187-190.

[17] Kurita N, Newman DD, Araguas-Araguas LJ, Aggarwal P. Evaluation of continuous water vapor $\delta^2H$ and $\delta^{18}O$ measurements by off-axis integrated cavity output spectroscopy. Atmos Meas Tech. 2012;5:2069-2080.

[18] Nelson DD, McManus JB, Herndon SC, Zahniser MS, Tuzson B, Emmenegger L. New method for isotopic ratio measurements of atmospheric carbon dioxide using a 4.3 μm pulsed quantum cascade laser. Appl Phys B. 2008;90:301-309.

[19] Mukai H, Iwami J, Tatematsu Y, Kajita Y, Endo F, Allison CE, and Francey RJ. About disagreement between inter-comparisons of isotopic ratio measurements for $CO_2$. Boulder, Colorado: 13th WMO/IAEA Meeting of Experts on Carbon Dioxide Concentration and Related Tracer Measurement Techniques. NOAA/ESRL Global Monitoring Division; 2005 September 19-22; Colorado, US.

[20] Werle P, Mucke R, Slemr F. The limits of signal averaging in atmospheric trace gas monitoring by tunable diode laser absorption spectroscopy. Appl Phys B. 1993;57:131-139.

403 [21] Coplen TB. Guidelines and recommended terms for expression of stable isotope-
404 ratio and gas-ratio measurement results. Rapid Commun Mass Spectrom.
405 2011;25:2538-2560.
406 [22] Werner RA, Brand WA. Referencing strategies and techniques in stable isotope
407 ratio analysis. Rapid Commun Mass Spectrom. 2011;15:501-519.
408 [23] Bowling DR, Sargent SD, Tanner BD, Ehleringer JR. Tunable diode laser
409 absorption spectroscopy for stable isotope studies of ecosystem-atmosphere $CO_2$
410 exchange. Agric For Meteorol. 2003;118:1-19.
411 [24] Weather, climate and earthquake information [Internet]. Tokyo: Japan
412 meteorological agency; [cited 2010 Oct 10]. Available from:
413 http://www.jma.go.jp/jma/indexe.html.
414 [25] Pataki DE, Alig RJ, Fung AS, Golubiewski NE, Kennedy CA, Mcpherson EG,
415 Nowak DJ, Pouyat RV, Romero-Lankao P. Urban ecosystems and the North
416 American carbon cycle. Glob Change Biol. 2006;12:2092-2102.
417 [26] NOAA Air Resources Laboratory, [Internet]. Silver Spring: Draxler RR, Rolph GD.
418 HYSPLIT (HYbrid Single-Particle Lagrangian Integrated Trajectory); [cited 2016
419 march 23]. Available from: http://ready.arl.noaa.gov/HYSPLIT.php.
420

1

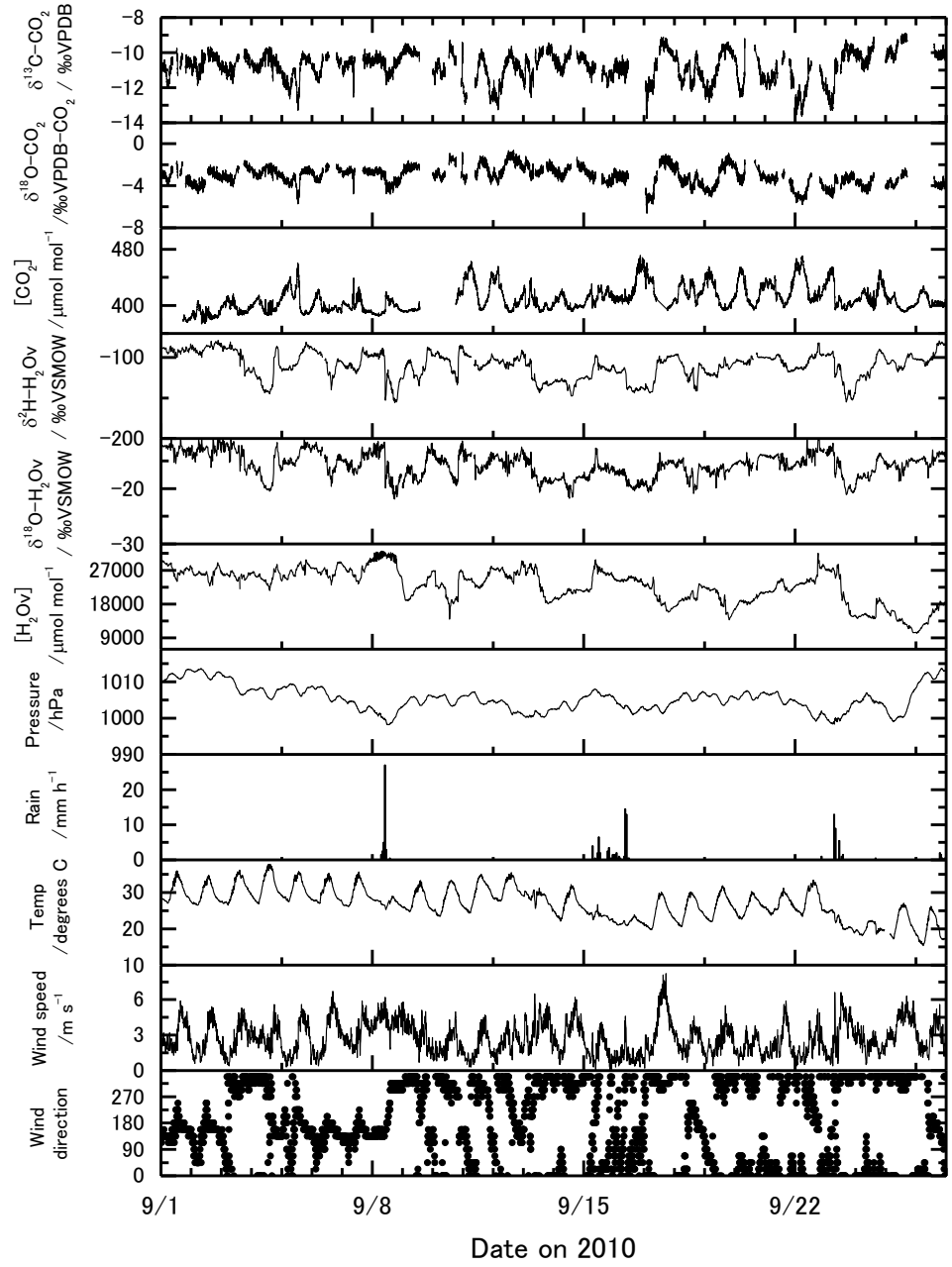


2

3 **Figure 1.** Concentrations and isotopic ratios of $CO_2$ and $H_2Ov$ measured using laser
4 spectrometers and the meteorological conditions in Nagoya, Japan in September 2010.
5 The meteorological conditions were obtained from the Nagoya Meteorological
6 Observatory.

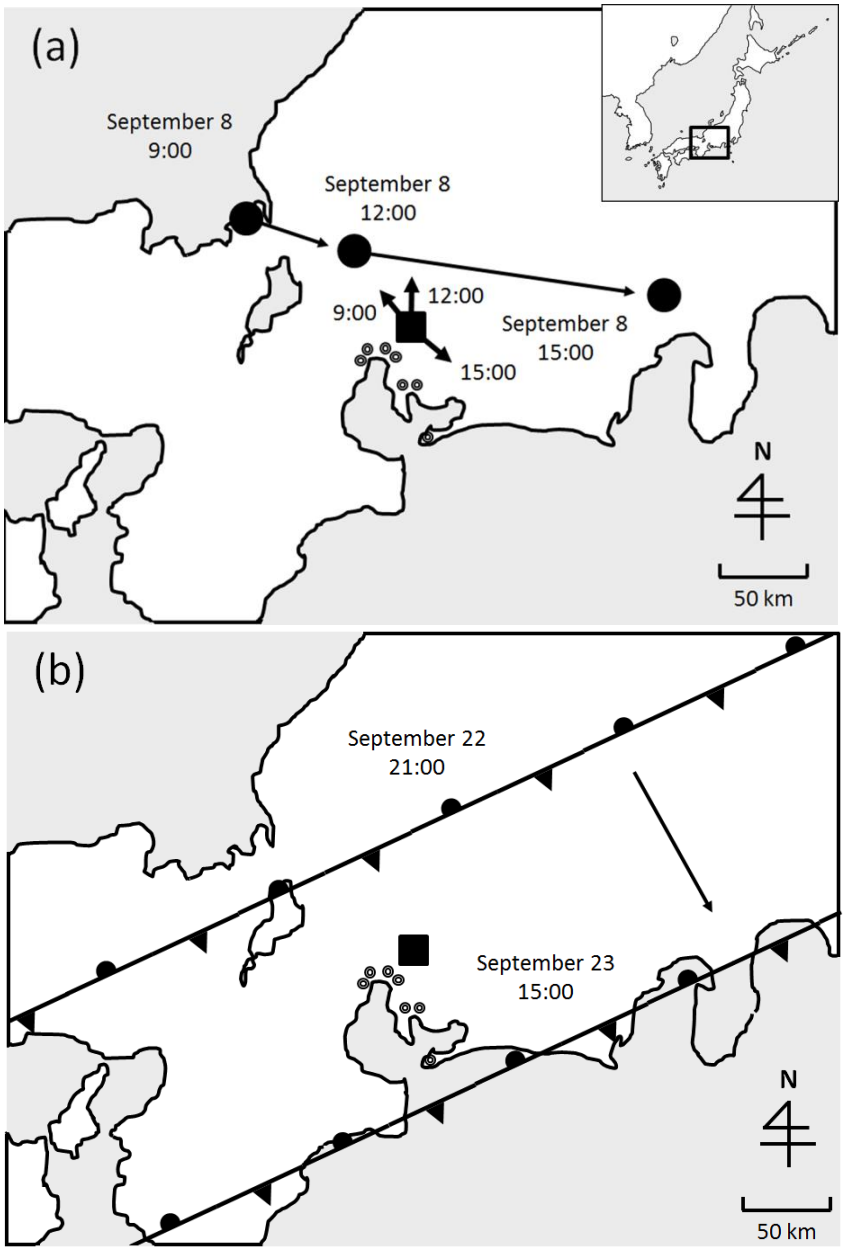


**Figure 2.** The tracks of (a) the typhoon and (b) the Akisame front across Nagoya in September 2010 reported by the Japan Meteorological Agency. The typhoon moved onto Honshu Island at 9 am on September 8, moved to the east after landing, and passed over the observatory. The Akisame front passed over the observatory on September 23. It stretched across Honshu Island from the east to the west, and moved from the northern to the southern side of the observatory. A filled square (■), a filled circle (●), and a double circle (◎) show the observatory and the positions of the center of the

typhoon and the thermal power stations, respectively. Arrows on the filled square show the wind directions at the observatory at the times shown in the figure.

19

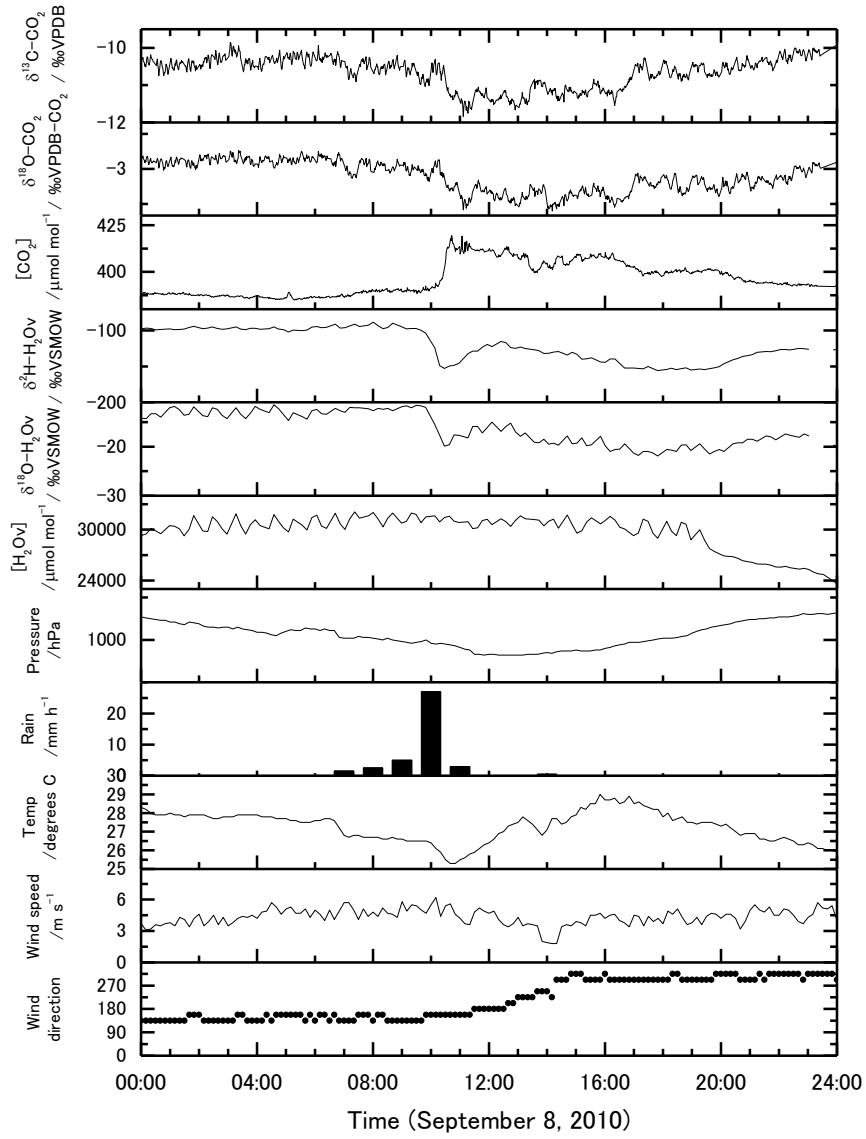


20

21 **Figure 3.** Concentrations and isotopic ratios of $CO_2$ and $H_2Ov$ measured using laser
22 spectrometers and the meteorological conditions in Nagoya on September 8, 2010. The
23 meteorological conditions were obtained from the Nagoya Meteorological Observatory.

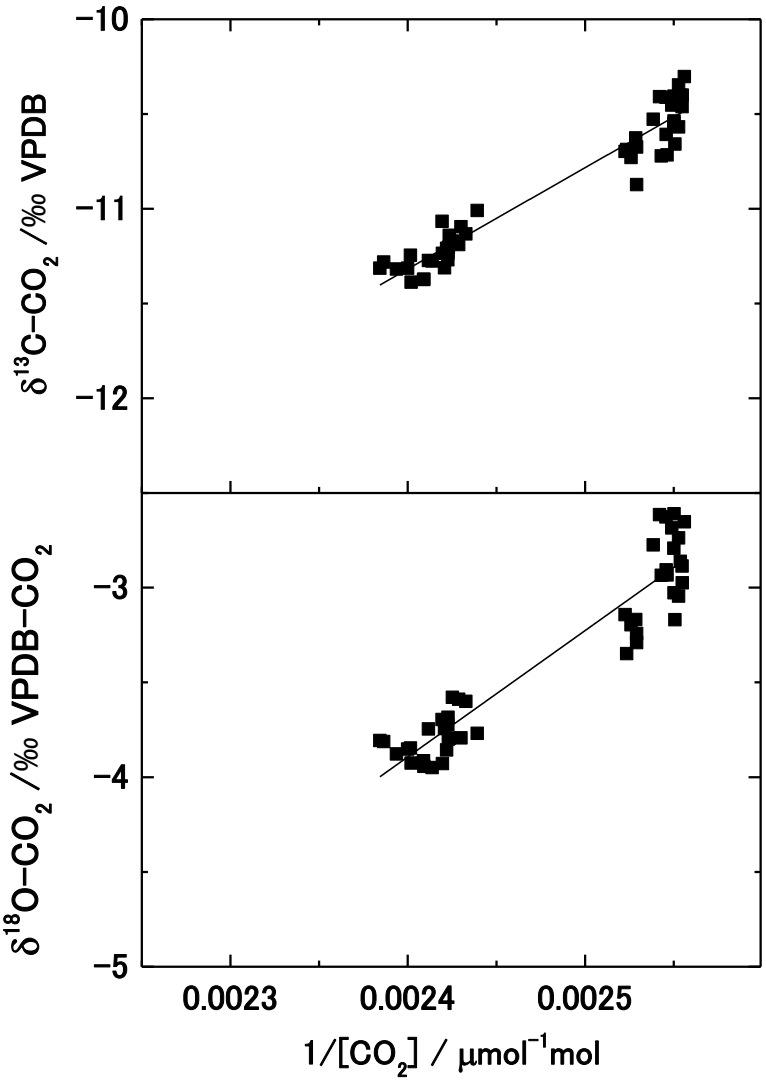


24

25

26 **Figure 4.** Keeling plots obtained using the $CO_2$ concentration and isotopic ratios of $CO_2$

27 (upper panel) $\delta^{13}C$ and (bottom panel) $\delta^{18}O$ from 10:00 to 11:00 on September 8, 2010,

28 when the typhoon passed over the observatory. The intercept values of the Keeling plots

29 are -24.2±0.5‰ for $\delta^{13}C$-$CO_2$ and -19.9±0.9‰ for $\delta^{18}O$-$CO_2$.

30

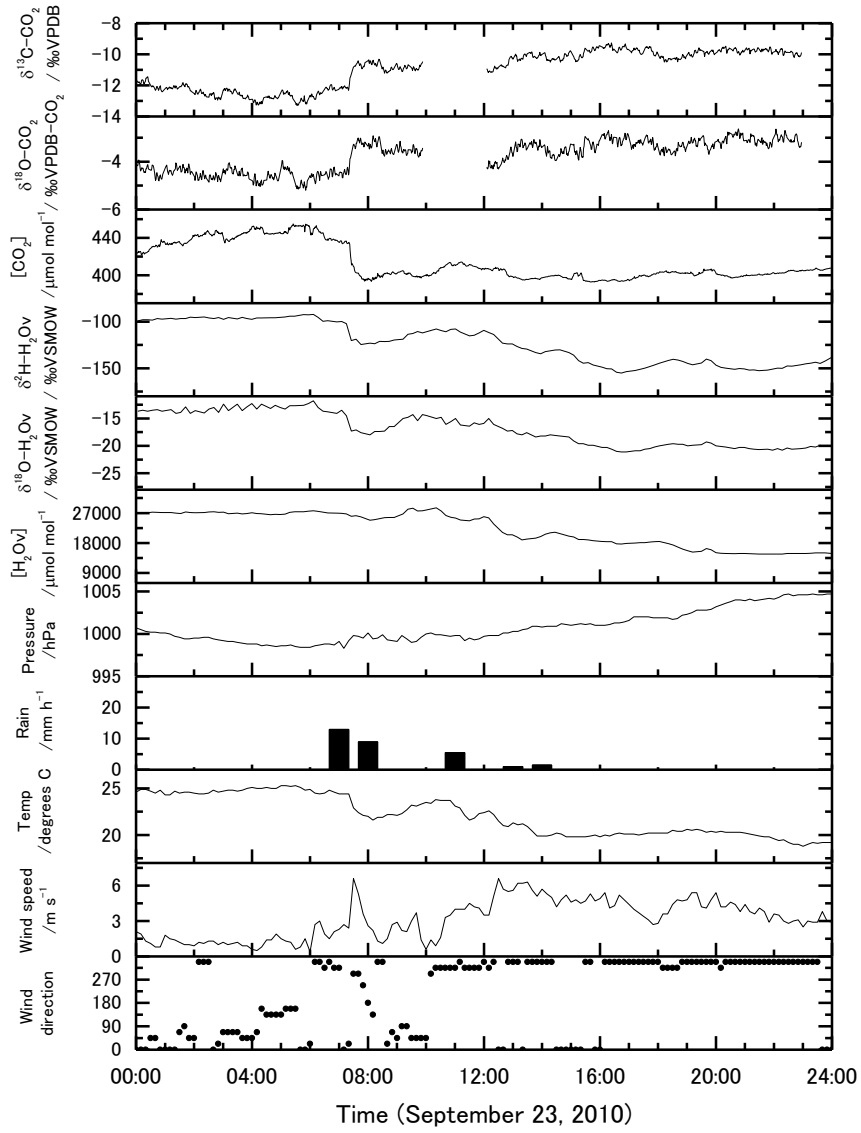


**Figure 5.** Concentrations and isotopic ratios of $CO_2$ and $H_2Ov$ measured using laser spectrometers and the meteorological conditions in Nagoya on September 23, 2010. The meteorological conditions were obtained from the Nagoya Meteorological Observatory.

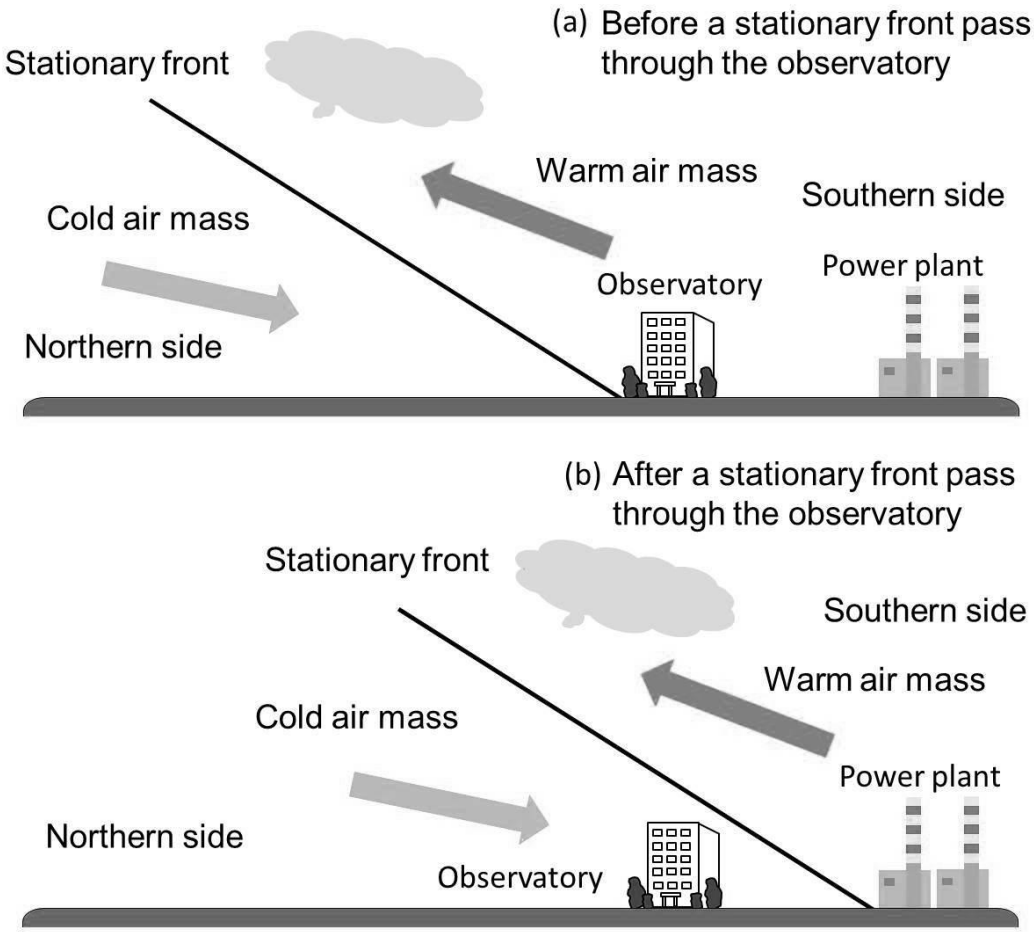


**Figure 6.** Positional relationship of the observatory, power plants, and the stationary front (a) before and (b) after the stationary front passed over the observatory.

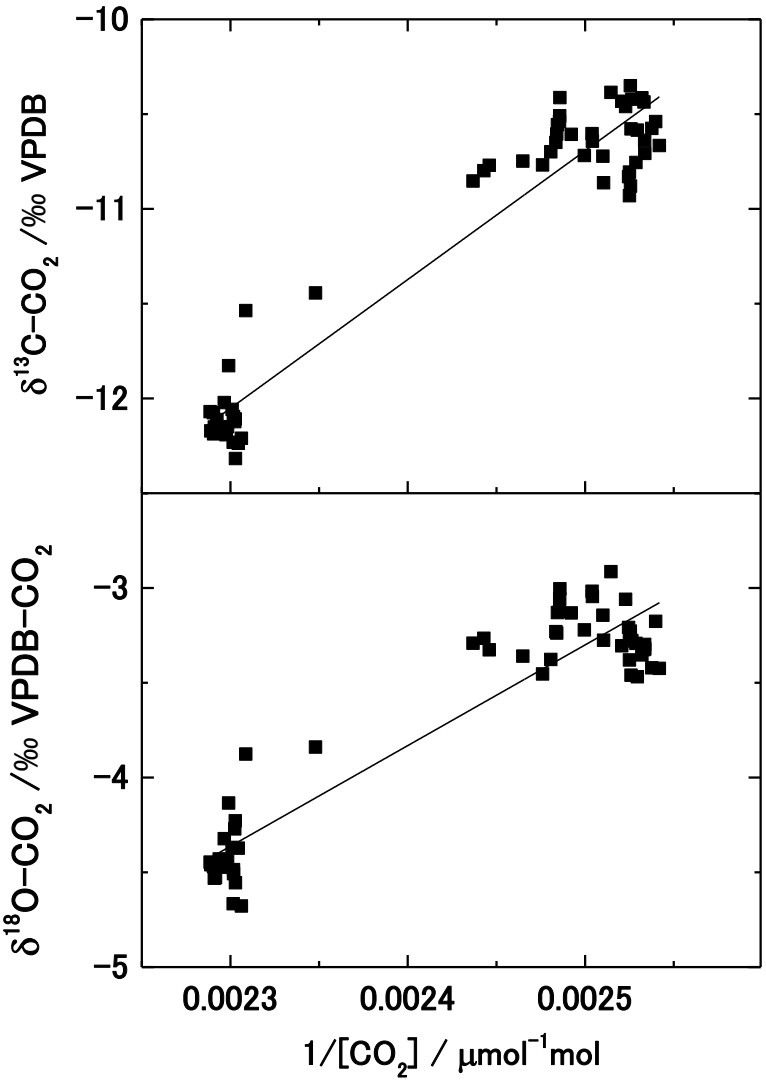


40

41 **Figure 7.** Keeling plots obtained using the $CO_2$ concentration and isotopic ratios of $CO_2$

42 (upper panel) $\delta^{13}C$ and (bottom panel) $\delta^{18}O$ from 7:00 to 8:00 on September 23, 2010,

43 when the Akisame front passed over the observatory. The intercept values of the

44 Keeling plots are -27.7±0.6‰ for $\delta^{13}C$-$CO_2$ and -16.6±0.6‰ for $\delta^{18}O$-$CO_2$.